

Charge exchange reactions on baryons and exotic low-mass narrow baryons.

B. Tatischeff* E. Tomasi-Gustafsson†

CNRS/IN2P3, Institut de Physique Nucléaire, UMR 8608, and Univ. Paris-Sud, Orsay, F-91405, France

Abstract

Narrow structures in baryonic missing mass or baryonic invariant mass were observed during the last ten years. Since their existence remains controversial, previously published data, measured with incident hadrons, are reanalyzed to add new pieces of information. This contribution gives further evidence to the existence of low mass exotic baryons, excited in charge-exchange reaction.

1 Introduction

Although already observed since several years, the genuine existence of narrow low-mass baryonic structures is often considered with skepticism. Various models on baryon spectroscopy describe, using q^3 configurations, the classical baryons up to $M=1.5$ GeV [1], namely those reported by the Particle Data Group [2]. Above $M = 1.5$ GeV arises the problem of missing resonances. Within the q^3 configuration models, there is no room for the narrow low-mass baryonic structures, which explains the skepticism.

This paper summarizes briefly the results where these structures were observed, and reanalyzes baryon induced charge exchange cross sections, in order to add information on these narrow baryonic exotic resonances. Indeed, the narrow structures were associated with multi-quark clusters, which is in accordance with the smaller signals in reactions involving incident leptons. Although studied for different physical motivations, therefore with statistical precision lower than the precision suitable for the present study, these results still add information concerning these structures.

The reanalyzed data are read, sometimes integrated over two or three channels, and kinematically transformed in order to draw histograms as functions of the missing mass, although they were published versus the energy loss or the final energy.

2 Brief recall of previous results

2.1 The SPES3 (Saturne) data

Only results concerning baryons will be discussed here. Previous experiments, performed at SPES3 (Saturne), thanks to good resolution and high statistics, exhibit narrow structures in different hadronic masses. Two reactions were studied [3, 4]: $p + p \rightarrow p + p + X$ (1) and $p + p \rightarrow p + \pi^+ + X$ (2). Structures were observed in the missing mass M_X of reaction (2), in the invariant mass M_{pX} of reaction (1), and in the invariant masses $M_{p\pi^+}$ and M_{π^+X} of reaction (2).

The observation of narrow structures in different conditions (reaction, incident energy, spectrometer angle, or observable) at the same mass (within ± 3 MeV) was considered to be a confirmation of their existence. The narrow structure masses observed are: 1004(α), 1044(β), 1094(γ), 1136(δ), 1173(ϵ), 1210(λ), 1249(η), 1277(ϕ), 1339(ν), and 1384 MeV. In parenthesis, the greek letters identify the structures shown in the corresponding figures. The vertical arrows in the following figures show the expected position for these narrow structures, on the basis of the previous findings. The two first masses, α and β lie below the pion threshold mass, which prove directly the exotic nature of these states. These results were published in: [4–6], respectively showing data in the missing mass region:

*e-mail : tati@ipno.in2p3.fr

†Permanent address: CEA, IRFU, SPhN, CEA/Saclay, 91191 Gif-sur-Yvette Cedex, France

$1.0 \leq M \leq 1.46$ GeV, $1.47 \leq M \leq 1.68$ GeV, and $1.72 \leq M \leq 1.79$ GeV. The narrow structures in the mass range $M_N \leq M \leq 1$ GeV, were also tentatively extracted [7].

Other signatures of narrow baryonic structures, were observed either in dedicated experiments or extracted from cross sections obtained and published by different authors studying other problems. They are quoted in [3–5] and will not be recalled here.

2.2 The $p(\alpha, \alpha')X$ reaction

Large statistics spectra of the $p(\alpha, \alpha')X$ reaction were obtained several years ago at SPES4 (Saturne) in order to study the radial excitation of the nucleon in the $P_{11}(1440$ MeV) Roper resonance. The experiment was performed with $T_\alpha=4.2$ GeV. A spectrum measured at $T_\alpha=4.2$ GeV, $\theta = 0.8^\circ$ [8] was built in the baryonic missing mass range: $1030 \leq M \leq 1490$ MeV. A first large peak around $\omega \approx 240$ MeV was associated with the projectile excitation, and a second large peak around $\omega \approx 510$ MeV was associated with the target excitation [8]. ω is the energy difference between the incident and the detected α particles. Above these large peaks lie narrow peaks, clearly observed, defined by a large number of standard deviations [9]. Another spectrum was measured at $T_\alpha=4.2$ GeV, $\theta = 2^\circ$ [10] which extended up to $M=1588$ MeV.

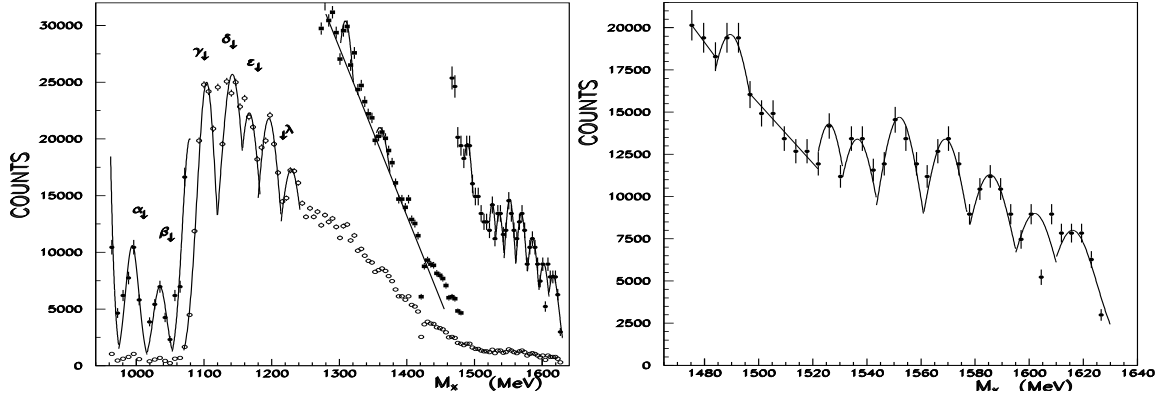


Fig. 1: Cross-section of the $p(\alpha, \alpha')X$ reaction at $T_\alpha=4.2$ GeV, $\theta = 2^\circ$ [10].

Fig. 1 shows this data. In both figures, the empty circles, which correspond to the scale, are the published number of events versus the missing mass. The full circles and full squares, in the left-hand part, show magnified data. Several peaks are observed above $M=1470$ MeV. The right figure shows an enhanced plot of this missing mass range ($\omega \geq 800$ MeV). The same situation, with many structures, is observed in the SPES3 data [5, 6], and all masses observed in both reactions have similar values. This fair concordance between the masses is observed using data originally obtained from experiments studied with different purposes, carried out by different physicists, studying different reactions with different probes and different experimental equipments.

3 New analysis of previously published charge-exchange reactions induced by baryons

A large number of charge-exchange reactions were studied in different laboratories, mainly at Saturne (SPES4 beam line), with the aim to study spin-isospin excitations. The corresponding missing mass data, range from the nucleon up to $\Delta(1232)$, therefore are quite convenient for the present study. A selected sample of these data is presented here, with the addition to the classical spectra of gaussians describing the narrow baryonic structures **having the previously determined masses** and a common width. The data are read, sometimes integrated over two or three channels and shown versus M_X .

3.1 The $p(p,n)\Delta^{++}$ reaction.

The differential cross-sections $d^2\sigma/dE_n d\Omega_n$ of the ${}^1H(p,n)X$ reaction were measured at LAMPF [11] at $T_p=790$ MeV, $\theta_n=0^\circ, 7.5^\circ, \text{ and } 15^\circ$. Fig. 2 shows the result for the two smallest angles. The full curves (small triangles) describe the theoretical calculations [12] performed with use of effective projectile-target-nucleon interactions. The open circles correspond to data integrated by two channels. A nice fit is obtained after introduction of the narrow resonances.

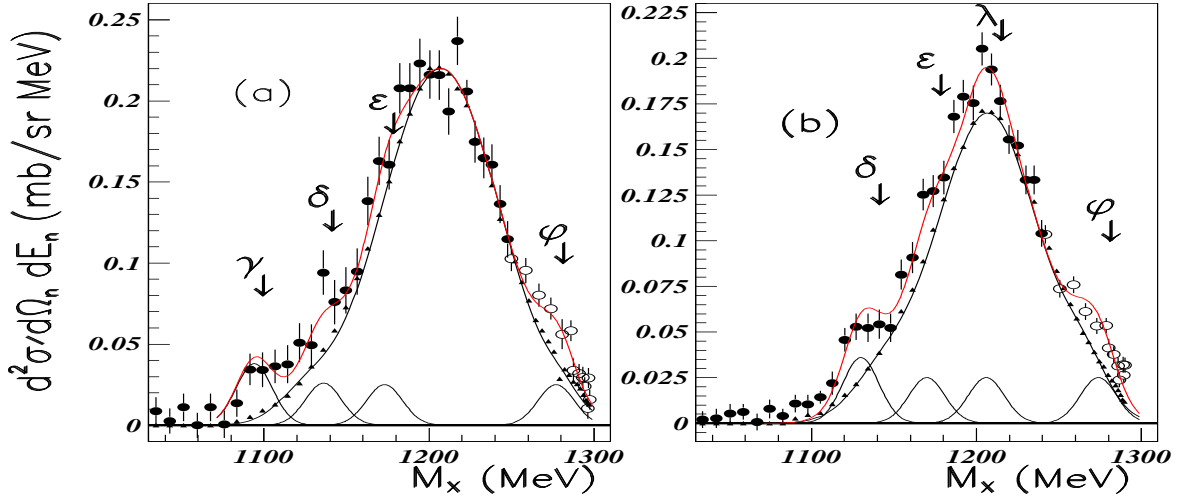


Fig. 2: (Color on line). Cross-section of the $pp \rightarrow n\Delta^{++}$ reaction at $T_p=0.79$ GeV. [11, 12]. Inserts (a) and (b) correspond respectively to $\theta_n=0^\circ$ and 7.5° .

3.2 The $p(d,2p)\Delta^0$ reaction.

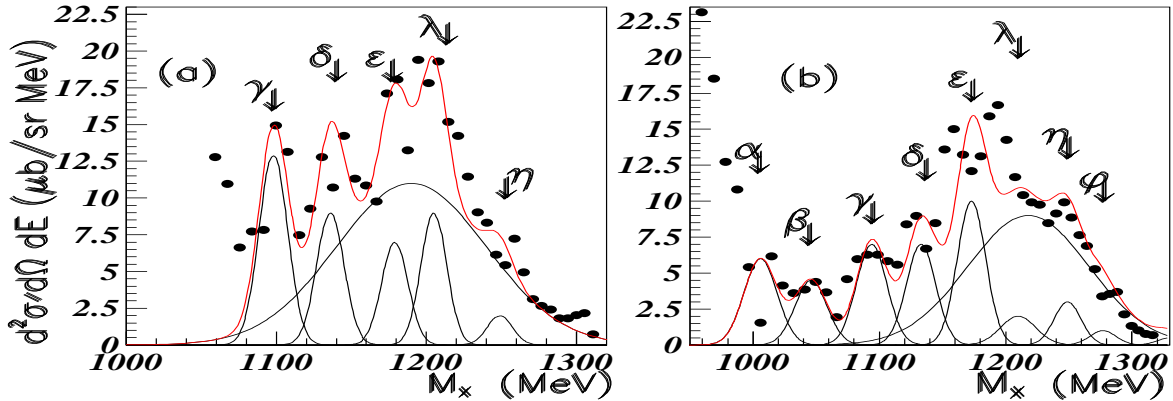


Fig. 3: (Color on line). Cross-section of the $p(d,2p)\Delta^0$ reaction at $T_d=2$ GeV $\theta = 0.5^\circ, \text{ and } 2.1^\circ$, respectively in inserts (a), and (b) [13–15].

The cross-section of the $p(d,2p)\Delta^0$ reaction was measured at the SPES4 spectrometer at Saturne, using 2 GeV and 1.6 GeV incident deuterons, at forward angles: $\theta_{lab} = 0^\circ, 0.5^\circ, 2.1^\circ, 4.3^\circ, \text{ and } 7.2^\circ$ [13–15]. Inserts (a) and (b) of Fig. 2 show the data respectively for $\theta=0.5^\circ$ and 2.1° . They exhibit an oscillating behaviour in the low part of the Δ missing mass range. The spectrum is well fitted by the masses of the narrow baryonic structures added to the broad Δ peak.

3.3 The $p(d)(^3\text{He},t)\Delta^{++}(X)$ reactions.

The cross-section of the $p(^3\text{He},t)\Delta^{++}$ reaction was measured at many incident energies, and spectrometer angles, not only with the SPES4 spectrometer at Saturne, but also in other experiments.

The old data from Dubna [16], at $T_p=2.39$ GeV, 4.53 GeV, and 8.33 GeV are not precise enough since their binning was equal to $\Delta E=25$ MeV. They are not reanalyzed here. The $^3\text{He}(p,t)\Delta^{++}$ reaction was studied at SPES1 (Saturne) at forward angle in the lab, with the motivation to reduce the direct graph and study the possible $(\Delta^{++},2n)$ component of the ^3He wave function [17]. The beam energy was $T_p=850$ MeV. These data correspond to $\theta_{lab}=6^\circ, 10^\circ,$ and 15° ; their cross-sections decrease fast with the increasing angle, therefore only the cross-section of the smaller angle is shown here, in Fig. 4. We observe that the structures exist, and are well fitted by the narrow structures if the data are shifted by $\Delta M=-9$ MeV. This shift may be due to a possible saturation of the spectrometer magnetic field: B, as small as $\delta p/p=6 \cdot 10^{-3}$, not taken into account, for large triton momenta for the SPES1 spectrometer: $p_t \approx 1.85$ GeV/c.

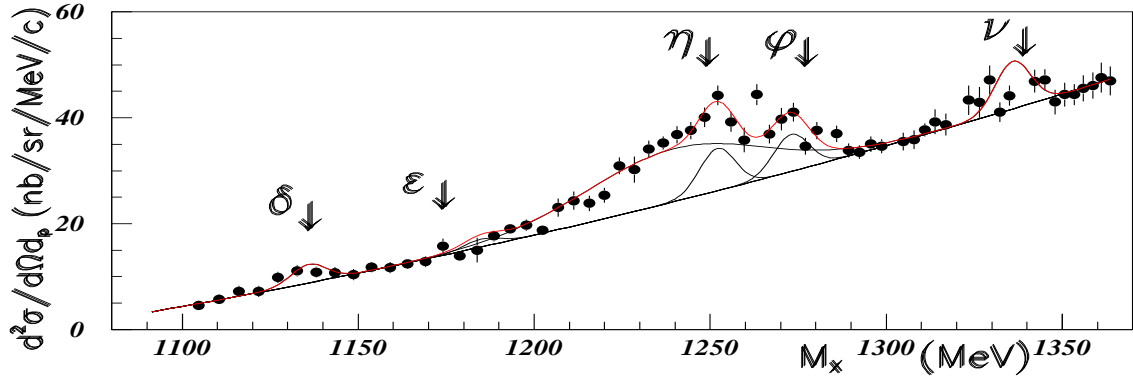


Fig. 4: (Color on line). Cross-section of the $^3\text{He}(p,t)\Delta^{++}$ reaction, at $T_p=850$ MeV, $\theta_{lab}=6^\circ$ [17] after a -9 MeV shift.

A selection of the data obtained at Saturne Spes4 beam line [18–20] is shown in Fig. 5.

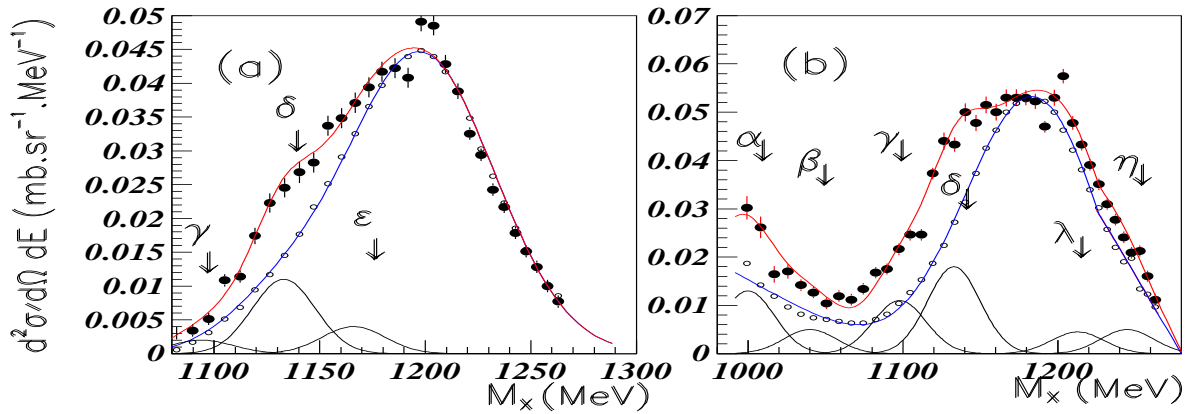


Fig. 5: (Color on line). Cross-sections of the $p(^3\text{He},t)X$ (insert (a)) and $d(^3\text{He},t)X$ (insert (b)) reactions at $T_{^3\text{He}}=2$ GeV, $\theta=4^\circ$ [18–20].

The calculation of the Δ^{++} contribution [20] includes the $A = 3$ form factors, as well as the quasi-elastic contribution and final state interaction for the reaction on the d target. The comparison between p and n targets, allows us to deduce that isospin $I = 1/2$ is favoured for these low mass baryonic structures.

The $^{12}\text{C}(^3\text{He}, t)$ reaction was studied at Saturne (SPES4 beam line) [21–23] at $T_{^3\text{He}}=2$ GeV, $\theta = 0^\circ$. A similar analysis shows that the addition of the narrow structures to the theoretical analysis performed by [22], allows to improve the fit to the data.

4 New reanalysis of several previously published charge-exchange reactions with incident light heavy-ion beams

4.1 Reactions on proton targets

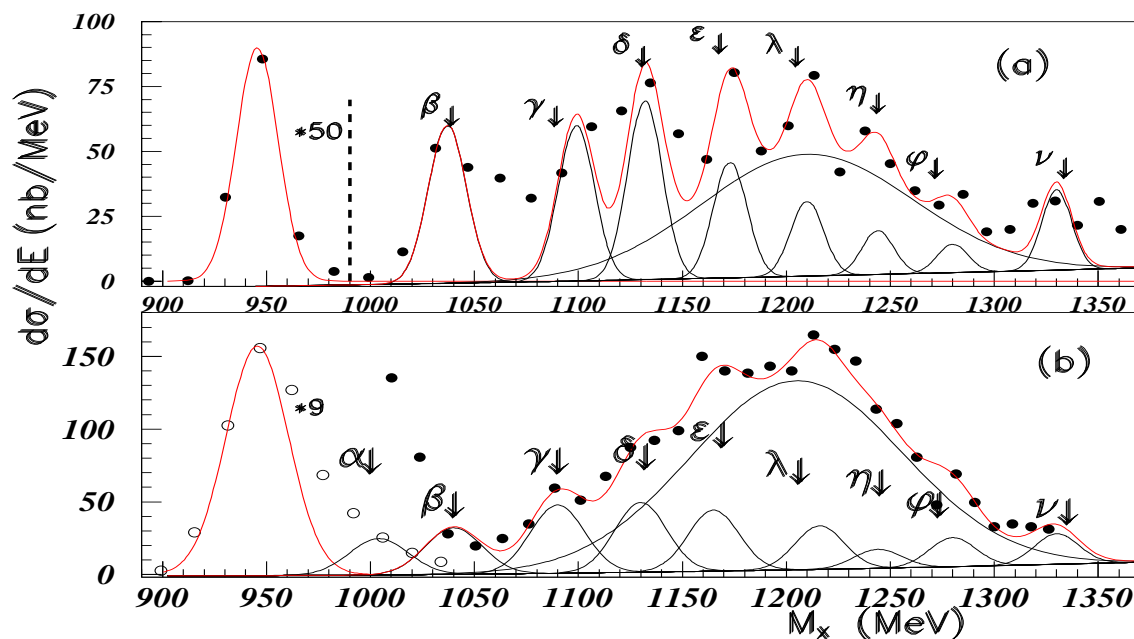


Fig. 6: (Color on line). Cross-sections: of the $p(^{12}\text{C}, ^{12}\text{N})\Delta^0$ reaction at $T_p=1100$ MeV/N $\theta = 0^\circ$ [24] in insert (a); of the $p(^{20}\text{Ne}, ^{20}\text{Na})\Delta^0$ reaction at $T_{^{20}\text{Ne}}=18$ GeV, $\theta = 0^\circ$ [24–27] in (insert (b)).

The $p(^{12}\text{C}, ^{12}\text{N})X$ reaction was studied at SPES4 (Saturne) using a ^{12}C beam of 1100 MeV/N at the spectrometer angle $\theta=0^\circ$ [24]. Fig. 6(a) shows these data, fitted with the Δ^0 peak and the structures previously observed. The important oscillatory behaviour is again very well fitted.

Fig. 6(b) shows the cross section of the $p(^{20}\text{Ne}, ^{20}\text{Na})\Delta^0$ reaction [24–27]. The comparison with the cross-section of the $p(^{20}\text{Ne}, ^{20}\text{F})\Delta^{++}$ reaction (not shown), allows us to conclude again that the first narrow baryonic structures have isospin $T = 1/2$, and those around $M = 1200$ MeV have isospin $T = 3/2$.

4.2 Reactions on light heavy ion targets

Two charge exchange reactions of light heavy-ion beams on ^{12}C target are shown in Fig. 7. Both were studied at Saturne SPES4 beam line, at $\theta=0^\circ$. Insert (a) shows the $(^{14}\text{N}, ^{14}\text{C})$ reaction at $T_{\text{beam}}=880 \cdot A$ MeV [28]; insert (b) shows the $(^{16}\text{O}, ^{16}\text{N})$ reaction at $T_{\text{beam}}=900 \cdot A$ MeV [29]. Here, an arbitrary background is introduced in order to simulate the inelastic scattering due to excitations of ^{12}C levels.

The same analysis, see fig. 8, is performed on the spectra of $^{27}\text{Al}(^{20}\text{Ne}, ^{20}\text{Na})X$ and the $^{27}\text{Al}(^{20}\text{Ne}, ^{20}\text{F})X$ reactions, measured at Saturne (SPES4), using a ^{20}Ne incident beam of $T=950$ MeV/A, at $\theta=0^\circ$ [28]. The introduction of narrow baryonic structures with masses previously determined, allows to reproduce the total spectra with the experimental oscillations.

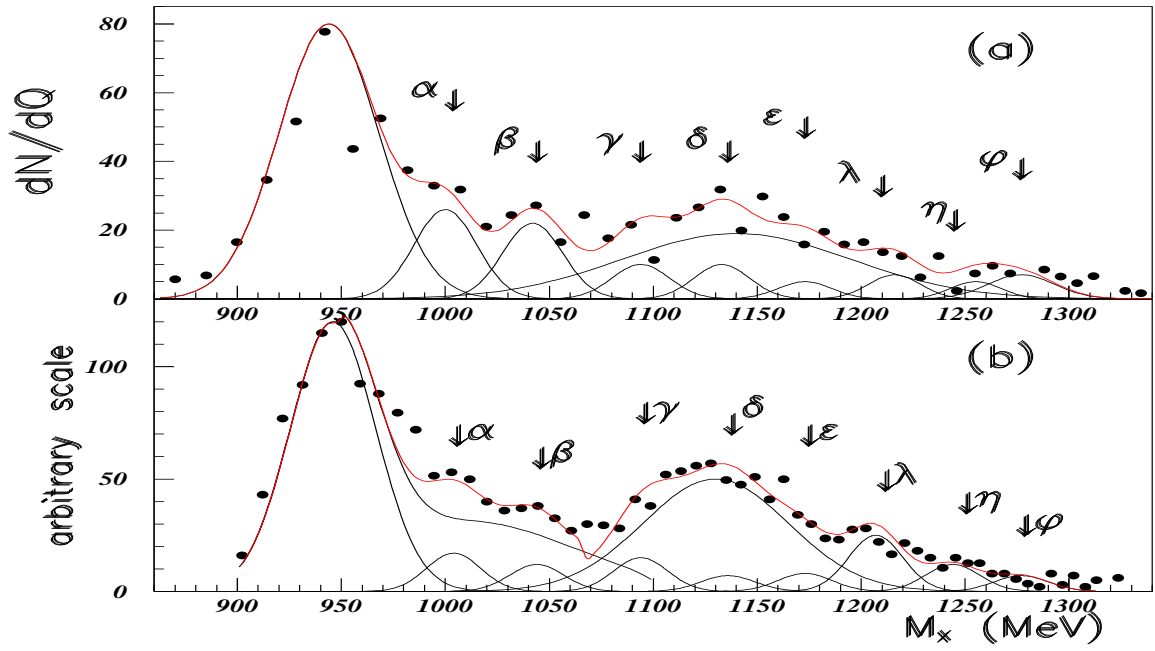


Fig. 7: (Color on line). Cross-sections at $\theta=0^\circ$: in insert (a) the $^{12}\text{C}(^{14}\text{N}, ^{14}\text{C})\text{X}$ reaction studied at Saturne (SPES4), at $T_{beam}=880 \cdot A$ MeV [28]; in insert (b) the $^{12}\text{C}(^{16}\text{O}, ^{16}\text{N})\text{X}$ reaction at $T_{beam}=900 \cdot A$ MeV [29].

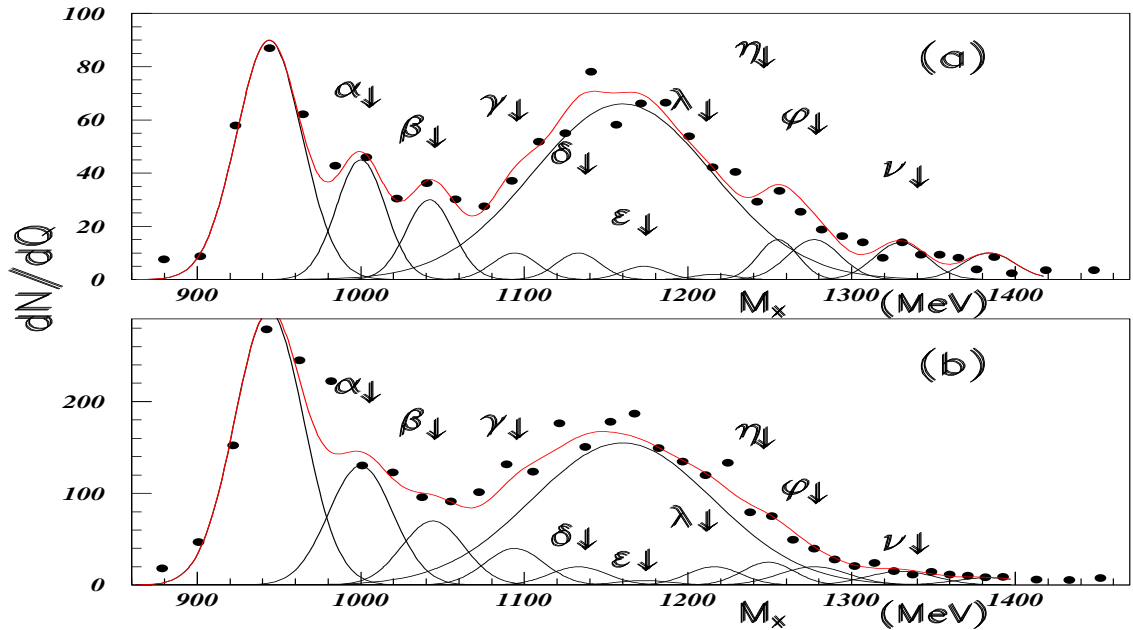


Fig. 8: (Color on line). Cross-section of the $^{27}\text{Al}(^{20}\text{Ne}, ^{20}\text{Na})\text{X}$ reaction (insert (a)), and $^{27}\text{Al}(^{20}\text{Ne}, ^{20}\text{F})\text{X}$ reaction (insert (b)). Both reactions were studied at $\theta = 0^\circ$, and $T_{beam}=950 \cdot A$ MeV. [28].

5 Conclusion

This work analyses different cross-sections of charge-exchange reactions induced by hadrons, in order to look to further signatures corresponding to the low mass narrow baryons previously observed. This paper does not pretend to give an exhaustive outline of all data where such signatures have been found, but focus on charge-exchange reactions.

These structures were associated with quark clusters [3, 4]; therefore reactions performed with

incident leptons, although allowing similar observations [30], lead to smaller signals than reactions performed with incident hadrons since the number of quarks involved in the reactions are reduced.

All reactions reanalyzed here were measured for another physical interest, therefore with a binning and statistics not optimized for the present study. So, there is here no attempt to study the mass range $950 \leq M \leq 1000$ MeV, although several spectra exhibit an excess of counting over the fits. Moreover, this missing mass region corresponds also to possible excitation of excited states in the nuclei, when composite targets are concerned.

In almost all spectra, clear structures are however observed, mainly below the region where the Δ starts to dominate the countings. This mass range concerns the structures at $M = 1004$ and 1044 MeV, particularly interesting since they are both located at masses lower than the threshold of possible pion-nucleon desintegration. The narrow baryonic resonances are observed in all missing mass range studied. The most noteworthy spectra, are those showing notable oscillations well fitted by the narrow structures. This concerns a large part of the reactions discussed previously, namely the spectra corresponding to the $pp \rightarrow p\pi^+ X$, $(d, 2p)X$, $(p, t)X$, $d(^3He, t)X$, $p(^{12}C, ^{12}N)X$, $^{12}C(^{16}O, ^{16}N)X$, $(^{20}Ne, ^{20}F)X$, and $(^{20}Ne, ^{20}Na)X$ reactions.

The comparison between final states with isospin $T=1/2$ and $T=3/2$, suggests to favor isospin $T=1/2$ for the lower narrow structure masses. These structures are more easily observed in reactions using isoscalar scattered particles such as α or deuterons.

These structures are clearly exotic since there is no room for them in the qqq configurations [1], since their width is smaller than the widths of "classical" PDG [2] baryonic resonances, and also since some masses lie below the pion threshold mass. They are naturally associated with precursor quark deconfinement. Therefore the quark and gluon degree of freedom is effective, even at very low energy, and must be taken into account. These conclusions are illustrated in Fig. 9 where the experimental masses of narrow baryonic structures are compared with masses calculated with help of a phenomenological mass relation [31] using two clusters of quarks at the ends of a stretched bag in terms of color magnetic interactions:

$$M = M_0 + M_1[i_1(i_1 + 1) + i_2(i_2 + 1) + (1/3)s_1(s_1 + 1) + (1/3)s_2(s_2 + 1)] \quad (1)$$

here i and s are isospins and spins of the two clusters. Notice that the formula allows degeneracy. We adjust the two parameters $M_0=838.2$ MeV and $M_1=100.3$ MeV in order to reproduce the masses, spins and isospins of N and Roper resonance $N^*(1440)$, and get the calculated masses of the other structures without any free parameter.

We conclude that the growing number of indications allow one to consider again the genuine existence of these structures as being a likely option.

References

- [1] S. Capstick and W.Roberts, Prog. Part. Nucl. Phys.**45**, 08241 (2000).
- [2] Particle Data Group, C. Amsler et al., Phys. Lett. **B667**, 1 (2008).
- [3] B. Tatischeff *et al.*, Phys. Rev. Lett. **79**, 601 (1997).
- [4] B. Tatischeff *et al.*, Eur. Phys. **A17**, 245 (2003).
- [5] B. Tatischeff *et al.*, Phy. Rev. **C72**, 034004 (2005).
- [6] B. Tatischeff *et al.*, Surveys in High Energy Physics, **19**, 55 (2004).
- [7] B. Tatischeff, Proceedings of the 16th International Baldin Seminar on High Energy Phys
- [8] H.P. Morsch *et al.* Phys. Rev. Lett. **69**, 1336 (1992).
- [9] B. Tatischeff and E. Tomasi-Gustafsson, Proceedings of the 17th International Baldin Seminar on High Energy Problems, Dubna 2004; arXiv nucl-ex/0411044.
- [10] H.P. Morsch, Proceedings of the Dixieme Journee Thematique de l'IPN d'Orsay (1995).

Parity	Config.	Mass (MeV)	Spin	Isospin	Calculation	Experiment
-	$(q\bar{q})-q^3$	1440.	1/2	1/2...5/2	1/2...5/2	Roper N* (1/2, 1/2) 1440
+	$(q\bar{q})^2-q^3$	1407	1/2...5/2	3/2	3/2	1384
+	$(q\bar{q})^2-q^3$	1340	3/2, 5/2	1/2, 3/2	1/2, 3/2	1339
-	$(q\bar{q})-q^3$	1306	1/2, 3/2	3/2	3/2	
+	\bar{q}^2-q^5	1273	3/2...7/2	1/2	1/2	1277
-	$(q\bar{q})-q^3$	1239	1/2	3/2	3/2	1249
+	$q-q^2$	1206	1/2, 3/2	1/2, 3/2	1/2, 3/2	(1210) 1173
+	$q-q^2$	1139	1/2	1/2, 3/2	1/2, 3/2	1136
-	$(q\bar{q})-q^3$	1106	1/2...5/2	1/2	1/2	1094
-	$(q\bar{q})-q^3$	1039	3/2	1/2	1/2	1044
+	$q-q^2$	1005	1/2, 3/2	1/2	1/2	1004
+	$q-q^2$	939	1/2	1/2	1/2	N 1/2 939

C A L C U L A T I O N
E X P E R I M E N T

- [11] D.L. Prout *et al.*, Phys. Rev. **C52**, 228 (1995).
- [12] C.A. Mosbacher and F. Osterfeld, Phys. Rev. **C56**, 2014 (1997).
- [13] C. Ellegaarde *et al.*, Phys. Rev. Lett. **59**, 974 (1987); *ibid* Phys. Lett. **B231**, 365 (1989).
- [14] T. S. Jorgensen, Cinquièmes Journées d'Études Saturne, Piriac, France, p 71 (1989).
- [15] T. Sams, Licentiaafhandling, Niels Bohr Institutet, Kobenhavns Universitet, (1990); T. Sams *et al.*, Phys. Rev. **C51**, 1945 (1995).
- [16] V.G. Ableev *et al.*, JETP Lett. **40**, 763 (1984).
- [17] B. Tatischeff *et al.*, Phys. Lett. **77B**, 254 (1978).
- [18] C. Ellegaard *et al.*, Phys. Lett. **154B**, 110 (1985).
- [19] T. Hennino *et al.*, Nucl. Phys. **A527**, 399c (1991).
- [20] B. Ramstein *et al.*, Eur. Phys. J. A **6**, 225 (1999).
- [21] D. Contardo *et al.*, Phys. Lett. **168B**, 331 (1986); D. Contardo, Thèse Univ. Claude Bernard, Lyon-1, n° 1557, (1984).
- [22] F. Osterfeld, B. Korfgen, P. Oltmanns, and T. Udagawa, Nucl. Phys. **A577**, 237c (1994).
- [23] T. Hennino *et al.*, Phys. Lett. **283B**, 42 (1992).
- [24] M. Roy-Stephan *et al.*, Nucl. Phys. **A488**, 187c (1988).
- [25] M. Roy-Stephan *et al.*, Nucl. Phys. **A482**, 373c (1988).
- [26] C. Gaarde, Annual Review of Nucl. and Part. Science **41**, 187 (1991).
- [27] M. Roy-Stephan, IPNO DRE 87-03 (1987).
- [28] D. Bachelier *et al.*, Phys. Lett. **172B**, 23 (1986).
- [29] C. Gaarde, Nucl. Phys. **A478**, 475c (1988).
- [30] B. Tatischeff and E. Tomasi-Gustafsson, arXiv:nucl-ex/0702005, and to be published.
- [31] P.J. Mulders, A.T. Aerts, and J.J. de Swart, Phys. Rev. **D19**, 2635 (1979).